


Review

Occurrence Regularity of Silt–Clay Minerals in Wind Eroded Deserts of Northwest China

Zhen Liu ^{1,2} , Hao Sun ^{1,2}, Ke Lin ^{1,2}, Cuiying Zhou ^{1,2,*} and Wei Huang ^{1,2}

¹ School of Civil Engineering, Sun Yat-sen University, Guangzhou 510275, China; liuzh8@mail.sysu.edu.cn (Z.L.); sunh65@mail2.sysu.edu.cn (H.S.); link35@mail2.sysu.edu.cn (K.L.); huangw226@mail2.sysu.edu.cn (W.H.)

² Guangdong Engineering Research Centre for Major Infrastructure Safety, School of Civil Engineering, Guangzhou 510275, China

* Correspondence: zhoucy@mail.sysu.edu.cn

Abstract: Wind erosion desertification is the most serious type of land degradation in Northwest China, so it is an important task for ecological management in the region. As the core of ecological management, soil quality is mainly affected by the presence of silt–clay content. Therefore, the grasp of its occurrence regularity is the key to controlling wind erosion desertification. At present, research on silt–clay contents is mainly independent in each local area and lacks integrity, which makes it difficult to meet the overall evaluation and planning requirements. To this end, this paper reviewed the related studies on the occurrence and control of wind erosion desertification in recent years and collected nearly 300 relevant silt–clay content data points. We studied the occurrence regularity of silt–clay content during the occurrence and treatment of wind erosion desertification and revealed the mechanism of silt–clay content in different processes. On this basis, the degree of wind erosion desertification in the major areas of Northwest China in the last five years was evaluated by calculations based on soil typing theory, and the fractal dimension interval (2.41–2.53) for the critical discrimination of desertification in these areas was obtained. The results showed that there were obvious distribution intervals of silt–clay content for different degrees of wind erosion desertification. Qualitative changes in soil quality during degradation ranged from light to moderate wind erosion desertification. The occurrence and control of wind erosion desertification were largely affected by the processes of silt–clay particles loss and aggregation. Among the three main treatment measures, biological measures enhanced silt–clay content most significantly. In this study, the occurrence regularity of silt–clay minerals in wind erosion desertification in Northwest China was revealed as a whole. This study provided a preliminary overall judgement of the dynamic evolution of wind erosion desertification, which provided a reference for the overall evaluation and global governance planning of wind erosion desertification in Northwest China.

Keywords: Northwest China; wind erosion desertification; silt–clay minerals; occurrence regularity; desertification control; fractal dimension



Citation: Liu, Z.; Sun, H.; Lin, K.; Zhou, C.; Huang, W. Occurrence Regularity of Silt–Clay Minerals in Wind Eroded Deserts of Northwest China. *Sustainability* **2021**, *13*, 2998. <https://doi.org/10.3390/su13052998>

Academic Editor: Adam Smoliński

Received: 29 January 2021

Accepted: 7 March 2021

Published: 9 March 2021

Publisher's Note: MDPI stays neutral with regard to jurisdictional claims in published maps and institutional affiliations.



Copyright: © 2021 by the authors. Licensee MDPI, Basel, Switzerland. This article is an open access article distributed under the terms and conditions of the Creative Commons Attribution (CC BY) license (<https://creativecommons.org/licenses/by/4.0/>).

1. Introduction

As one of the most serious types of land degradation in China, wind erosion desertification is widely distributed in a patchy or band-like pattern in Northwest China [1]. Its total area reaches 1,826,300 square kilometers, occupying 69.93% of China's desertified land area [2]. Such a wide distribution of wind-eroded deserts has triggered natural disasters such as sandstorms and sand raising, resulting in air and water pollution, which threaten people's lives and property security [3,4]. It has also led to coarsening soil texture and decreasing productivity, intensifying the human–land conflict, which seriously restricts the economic development of Northwest China [5]. As an important component of soil, clay minerals are formed by weathering and decomposition of primary minerals (silicate minerals) as hydrous layer aluminosilicates with particle size <2 μm [6]. Clay minerals

are characterized by high holding expansibility, great specific surface area, and a complex interlayer structure due to their extremely small particle size. These properties have a great influence on the physicochemical properties of the soil, such as its compactness, swelling, ion exchange, and fertility [7]. Since the weathering in Northwest China is not strong, clay minerals mainly exist in clay particles and partly in silt particles, therefore, the changes in silt–clay content can be used to grasp the rules and connections between the occurrence and control processes of wind erosion desertification in all of Northwest China. In this paper, the classification of silt ($<50\ \mu\text{m}$) and clay ($<2\ \mu\text{m}$) grains integrates the particle size and mineral composition. This information is necessary for the construction of ecological civilization and sustainable economic development in Northwest China.

Researchers have conducted several studies on sandy soils in major wind erosion desertification areas in Northwest China [8–12]. In terms of soil minerals, compositional analysis indicated that the degree of chemical weathering in these areas was low. The Nanjing Institute of Soil Research, Chinese Academy of Sciences, has zoned China by original material soil, the areas we studied (Northwest China) are all within the hydromica and hydromica-montmorillonite zones (1990 to present) [13,14]. The clay minerals in these areas are dominated by illite (60–70%), followed by montmorillonite and chlorite (10–15%) [15,16]. The 2:1 type clay minerals, such as illite and montmorillonite, affect the contents of potassium (K), phosphorus (P), and trace elements through homocrystalline substitution and adsorption [17]. These two clay minerals can also promote the agglomeration of organic matter through bonding, such as hydrogen bonding, ionic dipole forces, and van der Waals forces, and finally form organic-clay complexes. Since clay minerals exist mainly in silt–clay particles, the enrichment coefficients of P, K, and soil organic carbon (SOC) in silt–clay particles are much larger than those in very fine and medium coarse sands [18–20]. The content of silt–clay particles in the surface soil plays a major role in maintaining SOC, P, K and other nutrients [21]. These factors lead to the soil in Northwest China being characterized by high K, low P, and poor nitrogen (N) [22]. In terms of sandy soil particle size and physicochemical properties, researchers have focused on localized areas. In the Mu Us sandy land, topsoil particle size measurements indicated that fine sand was the major component of the soil matrix and that the soil had good sortability [23,24]. The differences in particle size characteristic values between different land types indicated that the effects of wind erosion on different land-use types were distinct and phased [25–27]. Soil physicochemical property analysis showed that the soil physicochemical properties changed regularly during wind erosion desertification [28]. As the degree of wind erosion desertification increased, the soil bulk weight increased significantly, and the components of soil water content, organic matter and total N decreased [29,30]. All these changes were significantly correlated with the changes in silt–clay content. Studies of the Alaska region revealed that during the reversal of desertification, along with the growth and development of vegetation, soil properties continued to increase and improve in structure, although the soil water content first decreased and then increased [31–33]. The thickness of the microbial crust formed on the surface layer of sandy soils gradually increased, and the soil had a tendency to develop gradually to deeper layers in the profile. At the same time, all the mineral elements necessary for plant growth showed an increasing trend, and the content of silt–clay particles continued to increase, while the content of silica (Si) gradually decreased, which was more favorable for plant succession and soil development [20,34–36]. Su et al. investigated the soils in areas with obvious desertification gradients in the Horqin sands and analyzed the physicochemical properties of different particle sizes [37–39]. The authors found that powdered clay particles had a lower soil bulk weight and a higher starting wind speed, capillary water holding capacity and nutrient content, while they had less of an effect on soil pH. For every 1% reduction in the content of clayey particles, the soil organic carbon (C) and total N contents will decline by 0.172 g/kg and 0.02348/kg, respectively [40]. The significant decreases in total soil porosity, capillary porosity, water holding capacity and soil nutrients during desertification were significantly and positively correlated with the changes in mineral content of clayey particles. The above studies were

conducted in terms of the occurrence or control process in wind erosion desertification. These studies revealed the interrelationships among the silt–clay particle contents, soil physicochemical properties, and dynamic changes in desertification in these specific study areas, and this information has positive effects on the evaluation of soil characteristics at different levels of desertification in these areas. However, the wind erosion desertification areas in Northwest China are widely distributed and large. There are differences and connections among wind-eroded deserts in different areas. The study of a single area cannot be accurately applied to the whole area affected by wind erosion desertification. Therefore, a large-scale and comprehensive evaluation of areas affected by wind erosion desertification needs further research.

In this study, we focused on the variation in silt–clay content. We collected and arranged nearly 300 relevant data points from different areas and stages of wind erosion desertification. By analyzing these data, we studied the occurrence regularity of silt–clay particles content in the process of wind erosion desertification and control. We also explained the law by the mechanisms that occurred. Based on the correlations among silt–clay content, soil volume fractal dimension and soil physicochemical properties, we calculated the critical interval of fractal dimension for the dynamic evolution of wind erosion desertification in major regions of Northwest China. This study can support the evaluation system of major deserts in Northwest China based on the silt–clay content. It can also provide a reference for the unified planning and management of areas affected by wind erosion desertification and promote the process of ecological civilization construction.

2. Occurrence Regularity of Silt–Clay Minerals in Wind Eroded Deserts

2.1. Occurrence Regularity of Silt–Clay Minerals in the Process of Wind Erosion Desertification

To study the changes in soil properties during the occurrence of wind erosion desertification, some researchers conducted long-term dynamic monitoring through scientific observations and research stations set up in the field. Other researchers used space instead of time to conduct their studies [41–44]. By analyzing soils in the desert-oasis transition zone with distinct desertification gradient characteristics, they obtained the silt–clay content in different stages of desertification. Since these studies are all superficial sandy soils within the last five years, no distinction is made between the sedimentation types of sandy soils. Tables 1 and 2 showed the relevant details of some soil samples from the references we have compiled and reviewed. In the currently available literature data, most of the data treat the components of the silt and clay particles as a whole and give the overall mineral composition. Therefore, the mineral composition given in Table 2 refer to the overall content of silt and clay particles. This does not affect the correctness of occurrence regularity or the comprehensive evaluation based on the content of silt–clay in this paper.

From the data in Tables 1 and 2 we can see that even though the wind eroded desertification areas in Northwest China are widely distributed, the mineral composition of silt–clay particles is approximately the same among all deserts due to the weak chemical weathering. This is also the basis on which we can evaluate the ecological construction of the entire Northwest China by the content of silt–clay minerals. At the same time, the soil texture is mostly loose single-grain structure because the soil type is dominated by aeolian sandy soil. By compiling the data from these studies, we obtained the distribution and degrees of silt–clay content in different regions.

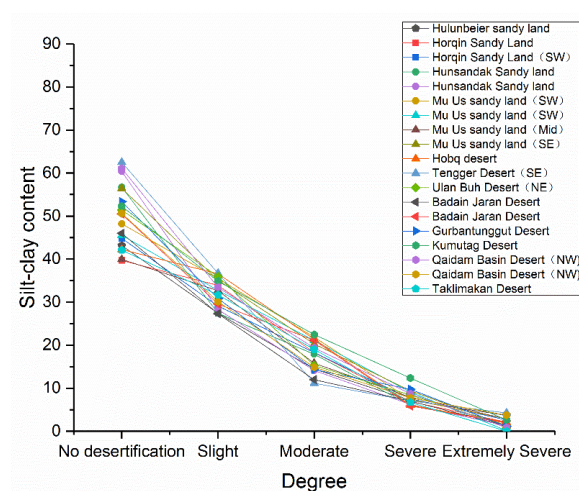
Table 1. Details of some soil samples (Data from reference [19,23,31,32,40–74]).

Desert (Abbreviation)	Sites of Desert	Coordinates	Number of Samples	Type of Samples
Hulunbuir Sands (HB)	Northeastern	115°31' E-126°04' E, 47°05' N-53°20' N	135	Aeolian sandy soil and chestnut soil
Horqin Sands (HQ1)	Southern	42°55' N, 120°41' E	90	Aeolian sandy soil and chestnut soil
	Southern	42°55' N, 120°42' E	72	
	Western	43°80' N, 119°83' E	80	
	Southwestern	42°15' N, 120°42' E	96	
	Southern	43°02' N, 119°39' E	48	
Horqin Sands (HQ2)	Eastern	101°59' E-104°12' E, 38°08' N-39°26' N	80	Aeolian sandy soil and grey brown desert soil
Hunsandak Sands (HD)	Southern	40°57' N-41°34' N, 114°10' E-115°27' E	36	Aeolian sandy soil
Mu Us Sands (MU1)	Southern	37°42' N, 107°42' E	60	Aeolian sandy soil and Sierozem
	Southeastern	110°04' E, 39°30' N	27	
	Southeastern	110°04' E, 39°30' N	54	
Mu Us Sands (MU2)	Southwestern	37°04' N-38°10' N, 106°30' E-107°41' E	175	Aeolian sandy soil and arenosols of quartisamment
	Western	37°55' N, 106°30' E	30	
	Southern	37°04' N-38°10' N, 106°30' E-107°47' E	54	
	Southern	37°04' N-38°10' N, 106°30' E-107°47' E	270	
Kubuqi Desert (KQ)	North	107°00' E-111°30' E, 39°30' N-40°41' N	144	Aeolian sandy soil and grey desert soils
UlanBuh Desert (UB)	Eastern	106°33' E-106°51' E, 39°40' N-40°13' N	121	Aeolian sandy soil and grey desert soils
	Eastern	40°09' N, 106°50' E	90	
Tengger Desert (TG)	Southeastern	37°30' N, 105°03' E	96	Aeolian sandy soil and brown desert soils
	Southeastern	37°32' N, 105°02' E	100	
	Southeastern	38°43' N, 105°31' E	70	
Badain Jaran Desert (BJ)	Southeastern	42°41' N, 102°08' E	72	Aeolian sandy soil, grey desert soils and grey-brown desert soils
	Southeastern	40°20' N, 97°36' E	180	
Qaidam Basin Desert (QB)	Southeastern	100°24' E-101°22' E, 35°27' N-35°47' N	45	Aeolian sandy soil
Kumutag Desert (KT)	Southeastern	38°20' N, 94°17' E	80	Aeolian sandy soil
Gurbantunggut Desert (GG)	Southern	44°40' N-45°56' N, 84°54' E-88°48' E	60	Aeolian sandy soil
Taklimakan Desert (TK)	Southern	35°17' N-39°30' N, 80°03' E-82°10' E	45	Aeolian sandy soil
	Southern	36°55' N-37°33' N, 82°36' E-83°12' E	60	
	Northern	40°86' N, 84°10' E	45	

Table 2. Components of silt–clay in different deserts (Data from reference [19,23,31,32,40–74]).

Desert	Soil Mineral Composition (%)									
	SiO ₂	Fe ₂ O ₃	MnO	TiO ₂	Al ₂ O ₃	CaO	MgO	K ₂ O	Na ₂ O	P ₂ O ₅
HB	72.4	2.63	0.05	0.59	11.93	2.32	0.89	2.93	2.49	0.05
HQ1	69.85	4.66	0.08	0.77	15.39	4.07	1.76	2.96	2.35	0.1
HQ2	71.15	2.81	0.05	0.61	12.21	2.32	1.05	2.87	2.5	0.1
HD	72.5	2.62	0.06	0.57	11.86	2.18	0.9	2.96	3.05	0.09
MU1	61.8	4.02	0.08	0.65	11.83	6.42	2.15	2.12	1.99	0.2
MU2	62.73	4.09	0.07	0.63	11.14	6.85	2.11	2.08	1.91	0.18
KQ	63.71	2.72	0.05	0.55	11.12	2.3	1	2.7	2.01	0.03
UB	61.56	4.11	0.08	0.64	11.94	6.8	2.2	2.11	1.97	0.16
TG	63.03	4.22	0.07	0.53	11.16	5.92	2.33	2.41	1.57	0.15
BJ	72.5	2.62	0.06	0.57	11.86	2.18	0.9	2.96	3.05	0.09
QB	59.49	3.69	0.07	0.47	10.67	8.99	2.87	2.4	2.41	0.17
KT	70.33	3.41	0.06	0.43	10.35	3.92	1.56	2.3	1.63	0.11
GG	58.63	4.14	0.11	0.57	10.5	4.46	2.61	2.48	1.86	0.19
TK	59.69	3.53	0.07	0.37	8.56	6.23	4.12	1.38	1.49	0.13

As shown in Figure 1, the distribution of silt–clay content in different areas without wind desertification ranged from 39.7% to 62.5%. The value was mainly influenced by the climate type, soil and moisture in the study areas, which showed zonal variations. Thus, the sites could be roughly divided into three categories: extremely arid areas (Taklamakan Desert, Kumutag Desert, and Qaidam Basin Desert), arid areas (Gurbantunggut Desert, Badain Jaran Desert, Tengger Desert, Kubuqi Desert, Ulan Buh Desert, and Mu Us Sands) and semiarid areas (Hunsandak Sands, Horqin Sands, and Hulunbuir Sands). This result is similar to the classification of Northwest China using elements in sand dunes [75]. As the degree of wind erosion desertification increases, the content of silt and clay particles in different regions decreases significantly, and the gap between regions is gradually reduced. The distribution of silt–clay content ranged from 22.73% to 36.66% when mild wind erosion desertification occurred and decreased to 14.32–21.84% when moderate wind erosion desertification occurred. The changes in silt–clay content in these two stages were relatively large, indicating that the soil structure and quality changed dramatically in this process but still had more obvious zonal characteristics. Therefore, the interval of silt–clay content in this stage could be used to judge whether wind erosion desertification occurred. When wind desertification developed to severe or extremely severe levels, the gap between different zones basically disappeared, and the silt–clay content declined to less than 12% or 4%, respectively, indicating that the soil almost completely lost its structure and fertility.

**Figure 1.** The silt–clay contents of different desertification levels in different areas (Data from reference [19,23,31,32,40–53,74]).

2.2. Occurrence Regularity of Silt–Clay Minerals in the Process of Different Wind Erosion Desertification Controls

2.2.1. Mechanical Sand Fixation Measures

Mechanical measures refer to the method of building sand barriers on the sand surface to achieve the effect of wind and sand fixation. The current studies have mainly evaluated the effectiveness and comprehensive benefits of sand barriers in terms of materials, deployment specifications, and deployment time [59–62,76]

In terms of material types, since sand barriers have a long history of development, there are many types of materials used to make them [77]. According to their sources, they can be divided into natural materials, such as wheat grass, sand willow, and clay, and new artificial materials, such as polylactic acid (PLA) and high-density polyethylene (HDPE). For different sand barrier materials, the evaluation of the barrier materials will be different if the focus of consideration is different (e.g., material cost, source, and durability). We evaluated the effect of different sand barriers from the viewpoint of the variation in silt–clay content collected the relevant data; the results are shown in Table 3.

Table 3. Different materials of sand barriers and the associated silt–clay contents.

Study Area	Sand Barrier Material	Silt–Clay Content
Mu Us Sandland [54]	Bare sandy land	0.139
	Salix psammophila	2.87
	PLA	1.837
Tengger Desert [59]	Bare sandy land	0.11
	Straw	3.44
	PLA	2.48
	Straw-PLA mix	3.04
Badain Jaran Desert [76]	Bare sandy land	1.15
	Dead Salix psammophila	3.45
	Straw	2.44
	Live Salix psammophila	6.68
	Sabina vulgaris	5.58

Table 3 shows that the natural materials with life activity (live balsam willow, etc.) can increase the content of silt–clay particles by 5.53%, which is much better than other materials. Natural materials without life activity and artificial materials can improve the content of silt–clay particles by 1.29–3.33% and 1.70–2.37%, respectively, indicating that they have a certain effect on wind erosion desertification, and the difference between them is small. It should be noted that vegetated living sand barriers are not preferred in some areas with severe moisture constraints.

For sand barriers of the same material, the different layout specifications and layout times are the main influencing factors for the change in silt–clay mineral content. As shown in Figure 2, the 1 m × 1 m sand barrier can increase the silt–clay content by 3.2–4.99%, which provides the best protection for wind-eroded sand. This result is basically consistent with the results obtained by measuring the change in erosion accumulation inside the sand barrier and wind velocity flow field simulation. With increasing deployment size, the enhancement of silt–clay content gradually decreases, and when the size increases to 3 m × 3 m, the enhancement of silt–clay content is only 2.91%. This result indicates that the sand barrier’s protective effect on wind eroded sand gradually decreases, but it is still higher than that of bare sand without a sand barrier. Considering the overall protection benefits of sand barriers, the smaller the size is, the higher the cost of sand barrier deployment is. Therefore, in areas with low wind erosion intensity, appropriately increasing the deployment size can achieve higher comprehensive benefits.

Figure 3 shows that all types of sand barriers can increase the silt–clay content by only 0.02–1.57% in the first two years of deployment, which is a limited improvement. As the deployment time increases, the dunes are fixed, and the microclimate inside the sand

barrier improves, leading to the gradual accumulation of silt–clay content to approximately 5%. After 6 years of grass square sand barrier deployment, there is a certain decline in the silt–clay content. This result indicates that the sand barriers made of natural materials will decay at a later stage of installation, which leads to a reduction in the protective effect.

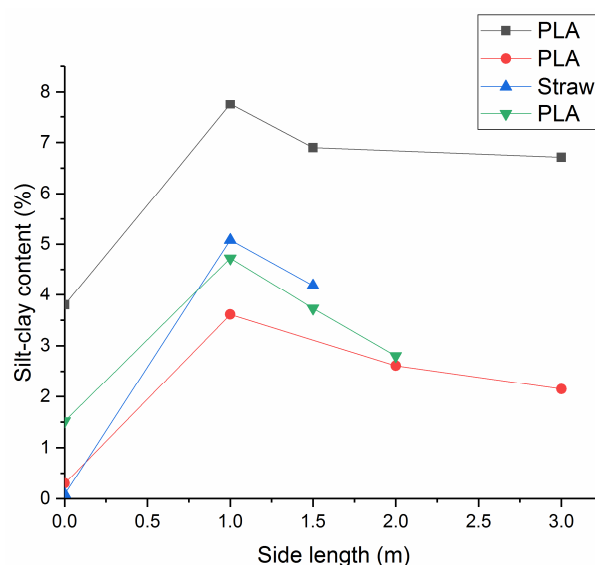


Figure 2. Different sizes of sand barriers and silt–clay content (Data from reference [59–62]).

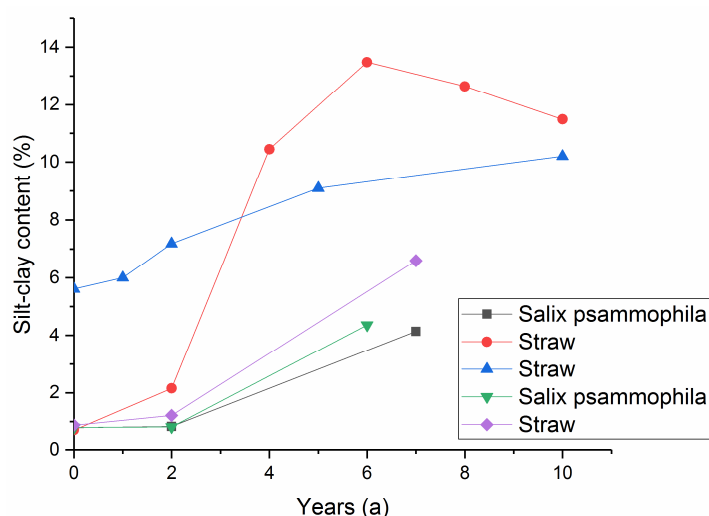


Figure 3. Different years of sand barriers and silt–clay content (Data from reference [54–58]).

Single mechanical sand fixation measures can improve the silt–clay content to some extent. However, whether by changing the materials, specifications, or age of placement, the increase in silt–clay content does not exceed 5%. This result indicates that single mechanical sand fixation measures can improve only the soil quality and control the wind erosion desert to a limited extent.

2.2.2. Chemical Sand Fixation Measures

Chemical sand fixation measures refer to mixing or spraying a chemical sand fixing agent into the surface soil of areas affected by wind erosion desertification [78,79]. By its own nature, it can directly or indirectly gel the soil sand particles and then form a consolidation layer [80,81]. As shown in Figure 4, it is the consolidation layer formed after the application of a new sand fixing agent called ADNB(The aqua-dispersing-nano-binder)

developed by our team [82]. Thus, the sand fixing agent can fix sand, resist wind erosion, and retain water [83–86].



Figure 4. Consolidation layer.

During this process, the silt and clay particles are bonded to form soil agglomerates of different sizes, and their content does not change significantly [87–90]. After the application of PistachioPVAc (polyvinyl acetate) and PistachioPAM (polyacrylamide) to windy sandy soil, the MWD (mean weight diameter) of soil aggregates increased from 0.06 mm to 1.38 mm [91]. Therefore, the current research focuses on the thickness, mechanical properties, durability, and weatherability of the consolidation layer [92–94].

2.2.3. Biological Sand Fixation Measures

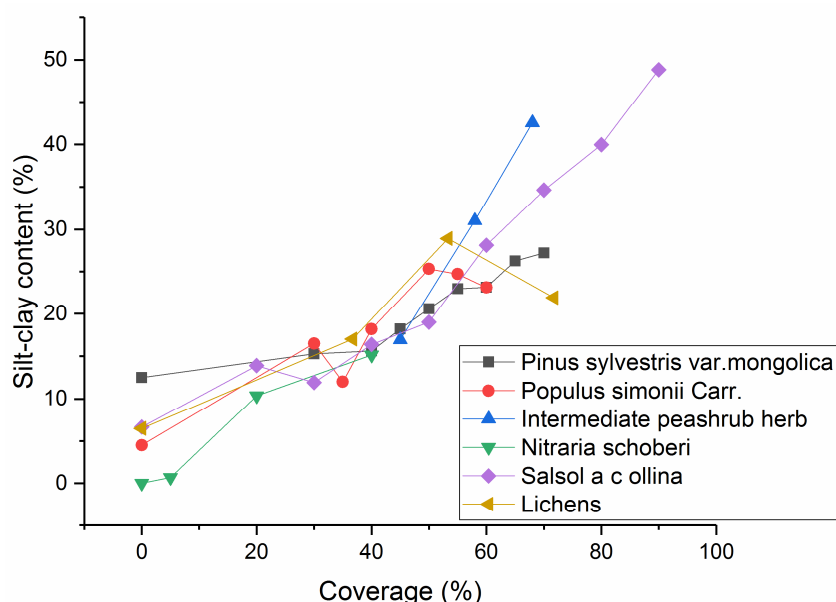
Biological measures mainly refer to plant sand fixation measures that use natural or artificial measures to restore vegetation, improve soil quality, and thus repair or rebuild the ecosystem [95]. To investigate the mechanism of plant measures in wind-eroded deserts and their optimal economic benefits, researchers compared the changes in silt–clay content in wind erosion desertification control areas from three aspects: different plant types, different vegetation covers and different planting years.

In terms of plant types, studies have shown that shrubs are much more effective at intercepting near-surface sand material than herbs and trees [96]. Desertification control practices and experiments by researchers in Northwest China have accumulated rich experience in recent decades [97]. They preferably selected the dominant cultivated species in arid areas, such as *Pinus sylvestris* var. *mongolica*, *Caragana korshinskii*, *Sabina vulgaris*, *Artemisia ordosica*, *Haloxylon ammodendron*, and *Salix cheilophila*. Most of these plants have similar characteristics. Their leaves are striped or linear to reduce transpiration and are more resistant to drought and wind erosion. The underground parts consist of a well-developed root system, which can effectively use groundwater and is resistant to sand burial. As seen in Table 4, all the different kinds of desertification vegetation have a greater enhancement of soil powder clay grain mineral content relative to the control sandy areas. In the areas with relatively good water and heat conditions, the increase in vegetation on the content of powdered clay particles can reach 31.58%. For different vegetation types in the same area, such as the Hulunbuir sands, the four vegetation species differed greatly, indicating that the selection of shrub species still needs to be analyzed and compared with the actual conditions and suitability of each area.

Table 4. Different vegetation species and silt–clay content.

Study Area	Vegetation Type	Silt–Clay Content	Study Area	Vegetation Type	Silt–Clay Content
Gonghe Desert [98]	Bare	1.5	Horqin Sand Land [99]	Bare	1.64
	<i>A. ordosica</i>	10.02		<i>Sabina vulgaris</i>	18.1
	<i>C. korshinskii</i>	10.22		<i>Ulmus pumila</i> l.	18.18
	<i>C. intermedia</i>	12.47		<i>Pinus sylvestris</i> var.mongolica	18.4
Otindag Desert [34]	Bare	1.74	Taklamakan Desert [100]	Bare	1.32
	<i>Stipa capillata</i>	22.3		<i>Caragana korshinskii</i>	28.9
	Fir	18.2		<i>Artemisia ordosica</i>	32.9
	<i>Caragana korshinskii</i>	11.7		<i>Haloxylon ammodendron</i>	28.1
	Littleleaf peashrub herb	8.5		<i>Salix cheilophila</i>	37

Studies on different vegetation covers showed that when the vegetation cover was low (<15%), the area was in a more serious stage of land desertification, and the silt–clay content was below 10% [47,63–67]. With the increase in vegetation cover, the silt–clay content gradually increased to 20–25% at a more moderate rate, indicating that the effect of the initial vegetation establishment on the silt–clay particle content was not significant. When the vegetation cover exceeded 60%, that is, when desertification was significantly improved, the soil quality of the area reached a solid stage of development, and the content of pink clay particles exceeded 30%, as shown in Figure 5.

**Figure 5.** Different coverage of vegetation and silt–clay content (Data from reference [47,63–67]).

Even for the preferred plant types, there was a mortality rate of approximately half during the growth process [101]. Therefore, the increase in planting time could not be considered as an increase in vegetation cover. Figure 6 shows that the silt–clay content increased to more than 20% in all major desertification areas after several decades of building artificial sand-fixing forest. The silt–clay content of the south-eastern edge of the Tengger Desert increased from 0% to 23.98% after 30 years of building an artificial sand-fixing forest, the powder clay content of the south-eastern edge of the Horqin sands

increased from 4.64% to 48.40% in 90 years under the protection of artificial camphor forests, and the powder clay content of the soils in the Mu Us sands increased from 12.40% to 27.19% in 24 years after camphor pine planting. However, it can also be clearly seen in the figure that almost every artificial sand-fixing forest had experienced different degrees of decline in silt–clay content during the development process. On the one hand, it may be due to the decrease of protection effect caused by the death of vegetation, on the other hand, it could be due to the depletion of soil nutrients caused by the growth of plants.

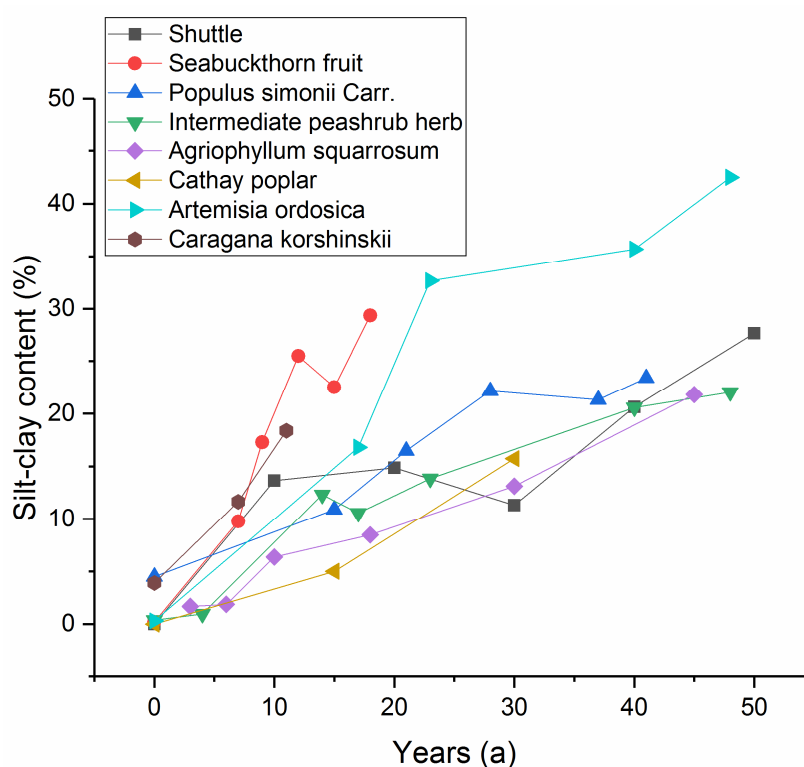


Figure 6. Different years of vegetation and silt–clay content (Data from reference [51,66,68–73]).

3. Mechanisms of Variation in Silt–Clay Content in Wind-Eroded Deserts

3.1. Mechanisms of Silt–Clay Content in the Process of Wind Erosion Desertification

During the process of wind erosion desertification, natural or human-induced factors lead to vegetation degradation, which exposes the topsoil to wind erosion. To investigate how soil particles with different grain sizes would respond to wind erosion, researchers compared the initial wind speed and wind erosion degree under net wind erosion for single-grain-size and mixed-grain-size sandy soils through indoor wind tunnel experiments [102–104]. Due to the different grading systems for soil particle sizes, the critical particle sizes obtained were slightly different. However, the conclusions all indicated that the larger grain size sand particles were difficult to erode due to higher gravity, and the silt and clay particles were difficult to erode due to their higher bonding force and the formation of wind-resistant clods; finally, the very fine sand was the easiest part to erode.

The movement modes and transport distances of different particle sizes also affected their response to wind erosion. As shown in Figure 7, after wind shear stresses were applied, the silt–clay particles with smaller masses and particle sizes moved in the air by suspension and over a longer distance. Soil particles smaller than 20 μm could even move thousands of kilometers [105,106]. This process is why the Taklamakan Desert can affect dustfall in the eastern coastal area of China [107]. Under the influence of wind shear stresses or other sand particles landing on the ground, very fine sands are transported in a small area on the surface by saltation. Medium coarse sands are characterized by larger masses and particle sizes, and wind shear stresses on their surfaces are slightly higher than

the critical shear stress for erosion; thus, they roll or slide along the surface in a creeping manner.

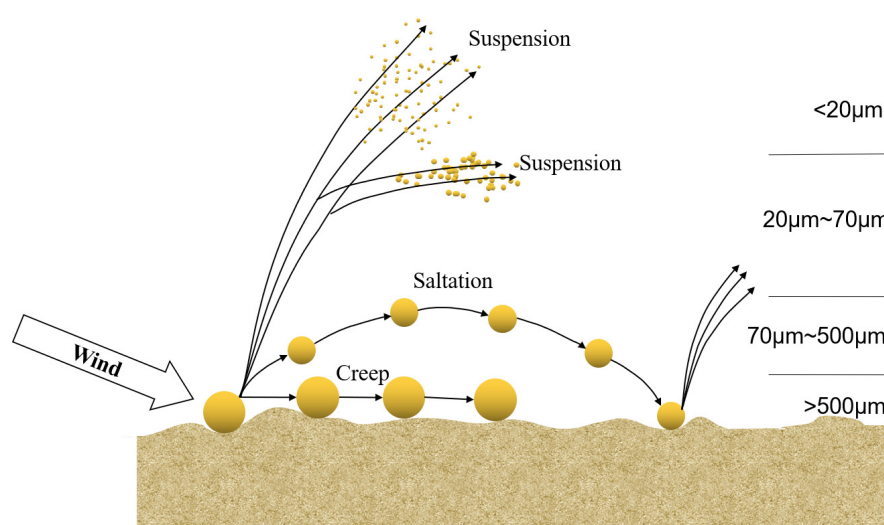


Figure 7. Different grain grade particle movements under the effects of wind erosion [108].

Combining the above studies on different grain grade particles in wind erosion, it can be concluded that although the silt–clay particles are not the most susceptible parts affecting by blowing, their transport distance under wind erosion is the longest. This result means that once wind erosion occurs, the corresponding particle size of silt–clay will be lost in the soil, while very fine sands and medium coarse sands will not cause the corresponding particle size to significantly decrease. In addition, the degradation of vegetation led to a reduction in the ability of microorganisms to refine soil particle composition. Therefore, the silt–clay mineral content reduction is most notable during wind erosion desertification.

However, because of the low erodibility of silt–clay particles, their contents can affect the mechanical properties and strength of the soil and thus control the wind erosion process [109]. Soil quality is influenced not only by mineral composition but also by the grading of soil [110,111]. In wind eroded desertification areas where sand grains account for more than 75% of the soil, an increase in the content of silt or clay grains can optimize the grading of soil, improve the soil structure and thus increase the soil's holding power, permeability and other properties [112,113]. As an intermediate stage in the weathering of primary minerals to clay minerals, the silt particles can be further weathered under certain conditions and release some of the nutrients such as K and P needed for plant growth [114]. Both in terms of particle size and mineral composition, the content of silt and clay particles has a significant impact on soil quality, therefore, the silt–clay content can be used as an indicator of the dynamic changes in wind-erosion deserts and the basis of desertification evaluation system [115]. Combined with the occurrence regularity of silt–clay content described in the previous section, we consider that the process of developing from light wind erosion desertification to moderate wind erosion desertification is a qualitative change in soil degradation. In this process, the silt–clay content decreases dramatically, and the soil structure changes dramatically. Therefore, we take 20–30% of the silt–clay content in this process as the interval used to identify desertification occurrence.

Soil particles are loosely bound in areas affected by wind erosion desertification. Wind erosion depletes gravelly soils by selectively eroding silt–clay particles, which are rich in nutrients and have a high holding capacity. At the same time, wind erosion destroys the soil structure and reduces the erosion resistance of the soil. This process occurs throughout wind erosion desertification, namely, soils where wind erosion desertification leads to silt–clay mineral loss are more susceptible to wind erosion.

3.2. Mechanisms of Silt–Clay Content in the Process of Different Wind Erosion Desertification Controls

3.2.1. Mechanical Sand Fixation Measures

As shown in Figure 8, the sand barrier embedding setting has a strong control capability on flowing dunes and reduces the dune movement rates, gradually transforming them into fixed dunes. Meanwhile, the surface roughness is increased by 400–600 times by changing the sub-bedding surface structure through sand barrier placement. When airflow passes through the sand barrier, it undergoes three main processes: eddy current deceleration, recovery acceleration, and blocking deceleration [116]. These processes enable the sand barrier to ultimately achieve a reduction in near-surface wind speed. Through actual wind–sand flow measurements and numerical simulations, researchers concluded that a 10–20 cm tall sand barrier can reduce the wind speed by 20–40% through two decelerations [58,117]. The sand barrier within this height range not only ensures that the original silt–clay particles within the sand barrier are not blown away but also saves materials to achieve high economic benefits. Under the effect of eddy current deceleration and sand barrier upper interception, silt–clay minerals partly settle and accumulate at the soil surface. Subsequently, under the action of airflow compaction, the silt–clay particles fill the voids in the soil structure, eventually improving the soil structure and significantly reducing the soil capacity. Due to the properties of silt–clay minerals, such as strong soil holding capacity, high porosity, and rich nutrient content, the physicochemical properties of surface soil, such as hardness and nutrient content, are somewhat improved.

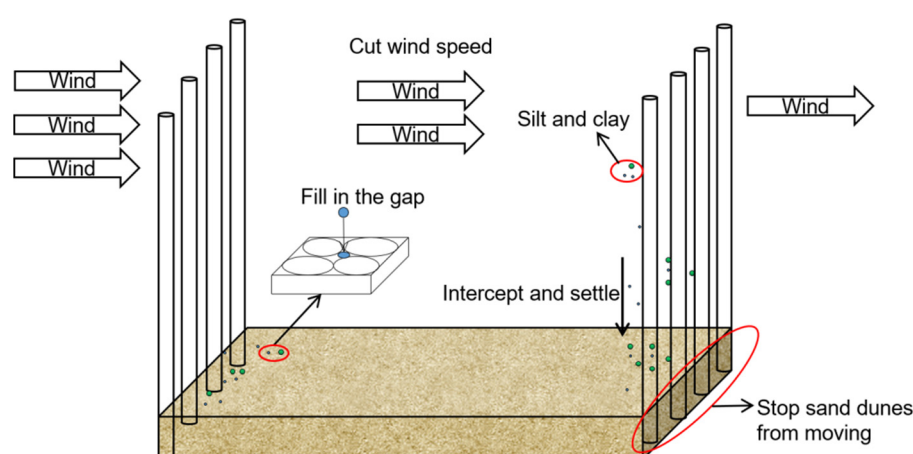


Figure 8. Mechanism of sand barrier sand fixation [116].

With the increase in sand barrier specification, the recovery acceleration phase is also prolonged, which leads to a decrease in the wind speed reduction ratio, resulting in an increase in the blowing effect on the surface silt–clay particles and a decrease in the protective effect [116]. However, it lessens the sand barrier deployment density and area, which weakens the interception effect of silt–clay particles in the air, leading to a decrease in the protection function [118]. The sand barrier installation time improvement promotes the accumulation of silt–clay particles and the decay of some sand barrier materials to enhance the microclimate inside the sand barrier and create a certain growth condition for the plant community, which gradually develops and stabilizes over time. During the process, the influence of the sand barrier on the silt–clay particle content also develops from the solitary action of the sand barrier itself to the joint role of the plant community and the sand barrier [119]. As a result, the increase in the mineral silt–clay mineral content gradually increases, but after the failure and decay of the sand barrier, there is a certain degree of decline.

Mechanical sand fixation measures can increase the silt–clay mineral content to some extent and thus improve soil quality. However, the effect of interception and sedimentation

determines only that mechanical measures cannot increase the silt–clay mineral content steadily and stably. The limited life span of sand barrier materials is another important factor to consider. Therefore, mechanical sand fixation measures are mainly used in areas affected by medium and heavy wind erosion desertification with poor environments and infertile soil or as pavement for biological sand fixation measures.

3.2.2. Chemical Sand Fixation Measures

Since there are tiny voids ($>8\ \mu\text{m}$) between particles on the surface of wind–sand soils, sand-fixing agent solutions with adhesive properties produce two main effects when sprayed onto the surface of quicksand [82], as shown in Figure 9. Droplets larger than the interparticle space are retained in the surface layer of sand, forming a layer of solidification with greater strength and not easy to blow after curing. Droplets larger than the interparticle space are retained in the surface layer of sand, forming a solid layer with greater strength that is not easy to blow after curing. Droplets smaller than the interparticle space penetrate into the sand body, forming a more stable and less blowing agglomerate under the influence of adhesion and intermolecular forces. Compared with single sand particles, the formed agglomerates have a larger mass and volume, which can increase the surface roughness and thus increase the starting wind speed; additionally, the agglomerates have the function of keeping the soil particles stable and improving the soil structure [71,120,121].

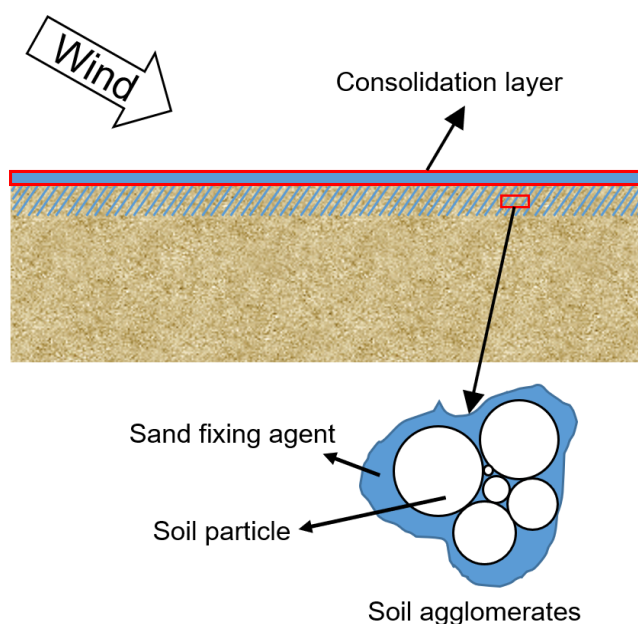


Figure 9. Mechanism of chemical measures for sand fixation [82,120,121].

Chemical measures maintain the silt–clay content by agglomerating them to reduce blowing rather than radically increasing the silt–clay content. With the passage of time, the curing agent gradually fails, and the protective effect on silt and clay particles also gradually disappears. However, chemical sand fixation has fast results, convenient construction, and other characteristics; thus, it is often used together with plant sand fixation measures to achieve fast and long-term sand fixation effects [122].

3.2.3. Biological Sand Fixation Measures

Plant sand fixation differs from the other two sand fixation measures because it has the closest interaction with the soil [123,124]. In biological and ecological terms, the ability of sand fixation or sand retention mainly depends on the distribution of branches and leaves in the near-surface layer. Plants with denser branches near the ground in the form of clumps can increase the roughness of the ground surface, thus weakening the wind motion at a certain height above the ground surface to weaken the wind motion reaching

the ground surface and ultimately reducing the migration loss of soil clay particles [70]. Therefore, among the three types of plants, i.e., trees, shrubs, and grasses, shrubs with dense branches are preferred over the poor weather-resistant herbaceous plants or trees with a single main stem.

As shown in Figure 10, the accumulation of litterfall in the topsoil cover during vegetation succession has the same protective effect on the soil. The longer the vegetation grows, the higher it grows and the more layers it covers, resulting in a better effect on weakening wind speed. The study on the Horqin sands showed that the weakening of the near-ground wind speed reached 60% when the vegetation cover reached 64%. The dense branches and foliage increased the dust-collecting effect of the plants, intercepting and accumulating the silt–clay particles from the wind–sand flow between plants or on the leeward side, forming a dune-like but immobile landform called nebkhas. Nebkhas can reduce sand abrasion effects on the plant community, thus playing an important role in fixing drifting sand and stabilizing the oasis ecosystem [16,125]. On the one hand, the underground root system of plants can serve as a reinforcement to consolidate the surrounding sand particles [72]. On the other hand, the organic compounds secreted by the rootstocks and the epidermal cells shed by the root crowns can refine the soil particles, promote the weathering of primary minerals and fundamentally increase the source of silt–clay minerals [72,126]. The decay of dead leaves on the surface increases the energy source of the soil microbial community, which contributes to microbial activity, reproduction, and organic matter accumulation, thus promoting the soil-forming action of sand and increasing the production potential [127].

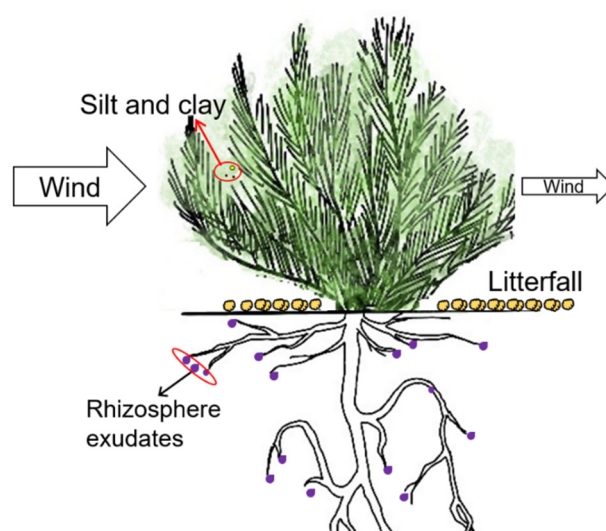


Figure 10. Mechanism of biological measures for sand fixation [72,128].

Although biological sand fixation measures cause changes in surface morphology, vegetation, etc., their essence is to deposit and significantly enrich soil silt and clay particles [128]. These changes have good ecological value, such as improving soil fertility and erosion resistance, which promote plant growth and community succession. They can also strengthen the stability of the soil–plant system, which creates a positive cycle between the plants and soil. In other words, soils with increased silt–clay minerals caused by biological measures are more conducive to vegetation growth and resistant to wind erosion [129]. Therefore, biological sand fixation can be considered the fundamental method of desertification control and the driving factor of evolutionary sand ecosystems.

4. Comprehensive Evaluation of Wind-Erosion Deserts Based on Silt–Clay Content

To accurately explore the changes in soil particle size distribution uniformity and soil texture at different stages of wind erosion desertification, the soil particle volume fractal

dimension model was introduced to calculate the fractal dimension (D) value and use it as a comprehensive index to evaluate the soil condition [130–132]. Its calculation formula is as follows:

$$\frac{V(r < R)}{V_T} = \left(\frac{R}{R_{\max}} \right)^{3-D} \quad (1)$$

Taking the logarithm of both sides of Equation (1) yields the following:

$$\log \left(\frac{V(r < R)}{V_T} \right) = (3 - D) \log \left(\frac{R}{R_{\max}} \right) \quad (2)$$

In the above equation, R_{\max} is the maximum particle size of soil in μm ; R is a specific particle size in μm ; $V(r < R)$ is the volume of soil particles with particle size less than R in cm^3 ; V_T is the total volume of soil particles in cm^3 .

A scatter plot is made with the left side of Equation (2) as the vertical coordinate and the right side as the horizontal coordinate. The linear regression fitting equation and fitting coefficient are obtained by adding the trend line according to the least squares method, and the slope of the fitting equation is $(3 - D)$ in Equation (2).

It can be seen from Equation (2) that the silt–clay particle content ($<50 \mu\text{m}$) has a large effect on the soil fractal dimension, and the researchers found a significant positive correlation with $<0.05 \text{ mm}$ particle content by correlation analysis. As mentioned earlier, during the development from mild to moderate wind erosion desertification, vegetation cover and dominant plants changed. Moreover, the content of soil powder and clay particles decreased dramatically, which made the soil structure change dramatically and was the process that qualitatively changed the soil quality. Therefore, we took the 20–30% silt–clay mineral content corresponding to this stage as the interval to judge the occurrence of desertification. Based on the data collected in the last five years, we studied the fractal dimension of the volume content of powdery clay minerals in areas affected by wind erosion desertification in Northwest China to determine the degree of desertification (see Table 5).

Table 5. Critical fractal dimensions of different wind erosion desertification areas.

Climate Type	Area	Critical Fractal Dimension	Silt–Clay Content
Semi-arid	Southern rim area of the Mu Us Desert [67]	2.527	19.74% silt 3.33% clay
	Mu Us Desert [64]	2.505	22.59% silt 6.25% clay
	South-west end of the Horqin Sandy Land [132]	2.532	21.09% silt 5.93% clay
Arid	Alxa Desert [52]	2.445	19.79% silt 2.7% clay
	Southeast edge of Qaidam Basin Desert [66]	2.4160	21% silt 4% clay
Hyperarid	Taklimakan Desert [19]	2.412	29.12% silt 1.10% clay

From Table 5, it can be seen that the critical fractal dimension varies less among different wind erosion desertification regions in Northwest China, and all of them are distributed between 2.41 and 2.53. At the same time, the D values showed a decreasing trend from the semiarid to extremely arid regions as shown in Figure 11.

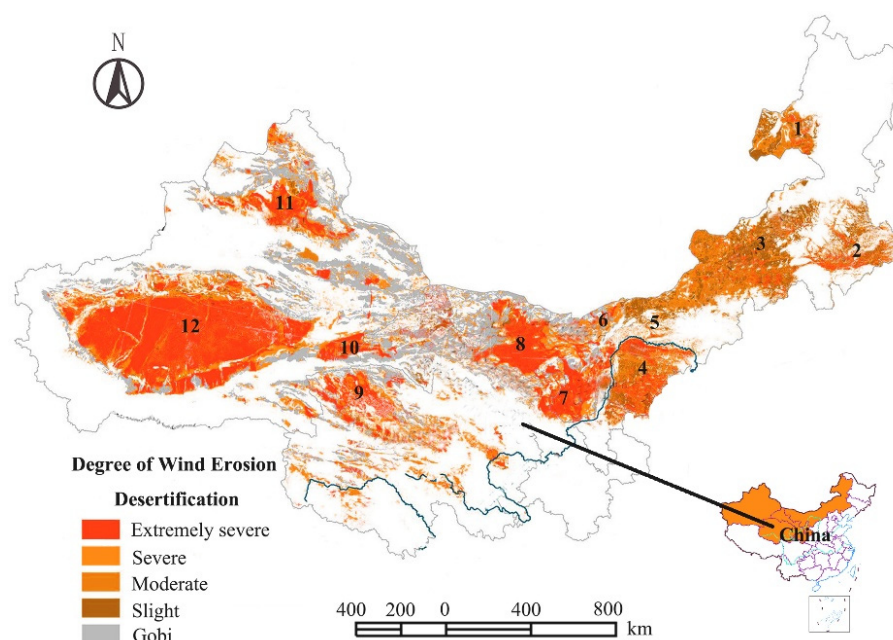


Figure 11. Distribution of wind erosion desertification in Northwest China (1. Hulunbuir Sandy land 2. Horqin Sandy land 3. Hunsandak Sandy land 4. Mu Us Sandy land 5. Kubuqi Desert 6. Ulan Buh Desert 7. Tengger Desert 8. Badain Jaran Desert 9. Qaidam Basin Desert 10. Kumutag Desert 11. Gurbantunggut Desert 12. Taklamakan Desert, Data from reference [2,4]).

The D value is significantly correlated with soil quality indicators such as soil organic matter, total N, and bulk weight, and the D value can be used as a comprehensive indicator to respond to soil texture and then judge the degree of soil degradation. Therefore, we suggest that 2.41–2.53 would be the critical interval for whether wind erosion desertification occurs in major areas of Northwest China. When the fractal dimension falls below 2.41 and tends to decrease, it indicates that moderate wind desertification has occurred in the region; when the fractal dimension ranges from 2.41 to 2.53, it means that the soil quality of the region is experiencing dynamic changes in moderate or mild wind desertification, and corresponding measures are needed to suppress the increase of wind desertification. Finally, when the fractal dimension is higher than 2.53, it reflects that the soil quality of the area is good and wind desertification has not yet occurred.

5. Conclusions

This paper reveals the overall pattern of silt–clay minerals in wind-eroded deserts through a review of the literature and data analysis. It is shown that the occurrence and control of wind erosion desertification is largely a process of loss and aggregation of silt–clay minerals. Qualitative changes in soil quality during degradation ranged from light to moderate wind erosion desertification; thus, the results provide an idea to clarify the overall evolutionary characteristics of wind-erosion deserts in Northwest China. Based on the obtained occurrence regularity the critical values of fractal dimension for the occurrence of wind erosion desertification in major areas of Northwest China in the past five years were calculated by using soil volume fractal theory. The change trend was analyzed from the overall perspective by combining the climate types. The fractal dimension interval (2.41–2.53) for the critical discrimination of wind erosion desertification in Northwest China was obtained. The content of silt–clay minerals in soil can be used as a quantitative assessment standard for soil structure and quality in areas affected by wind erosion desertification in Northwest China and then can be used to judge the dynamic evolution process of desertification. This information provides a reference for the overall evaluation and global planning of desertification in Northwest China.

Author Contributions: Z.L.: Methodology, Formal analysis, Writing—Review & Editing, Project administration. H.S.: Methodology, Formal analysis, Data Curation, Writing—original draft, Visualization. K.L.: Writing—review & editing, Data Curation, Visualization. C.Z.: Writing—review & editing, Supervision. W.H.: Writing—review & editing, Formal analysis. All authors have read and agreed to the published version of the manuscript.

Funding: This research was funded by National Key Research and Development Program of China (Grant No. 2017YFC1501203 and 2017YFC0804605 and 2017YFC1501201), the National Natural Science Foundation of China (Grant No.41977230), Key Project of Applied Science & Technology Research and Development of Guangdong Province, China (Grant No. 2015B090925016 and 2016B010124007), and Guangzhou Science and Technology Project (Grant No. 201803030005). The authors would like to thank the anonymous reviewers for their very constructive and helpful comments.

Institutional Review Board Statement: Not applicable.

Informed Consent Statement: Not applicable.

Data Availability Statement: The data presented in this study are available in the corresponding references.

Conflicts of Interest: The authors declare no conflict of interest.

References

- Gou, F.; Liang, W.; Sun, S.; Jin, Z.; Zhang, W.; Yan, J. Analysis of the desertification dynamics of sandy lands in Northern China over the period 2000–2017. *Geocarto Int.* **2019**, *10*, 12–26. [\[CrossRef\]](#)
- A Bulletin of Status Quo of Desertification and Sandification in China. State Forestry Administration: Beijing, China, 2014; p. 22.
- Zhang, J.G.; Xu, X.W.; Zhao, Y.; Lei, J.Q.; Li, S.Y.; Wang, Y.D. Effect of shifting sand burial on soil evaporation and moisture–salt distribution in a hyper-arid desert. *Environ. Earth Sci.* **2016**, *75*, 1–10. [\[CrossRef\]](#)
- Guo, Z.; Huang, N.; Dong, Z.; Van Pelt, R.S.; Zobeck, T.M. Wind erosion induced soil degradation in Northern China: Status, measures and perspective. *Sustainability* **2014**, *6*, 8951–8966. [\[CrossRef\]](#)
- Tao, W. Aeolian desertification and its control in Northern China. *Int. Soil Water Conserv. Res.* **2014**. [\[CrossRef\]](#)
- Mueller, K.T.; Sanders, R.L.; Washton, N.M. Clay minerals. *eMagRes* **2014**. [\[CrossRef\]](#)
- Matsui, K.; Watanabe, T.; Kussainova, M.; Funakawa, S. Soil properties that determine the mortality and growth of *Haloxylon aphyllum* in the Aral region, Kazakhstan. *Arid L. Res. Manag.* **2019**, *33*, 37–54. [\[CrossRef\]](#)
- Liu, W.; Lü, S.; Wang, T.; Yan, R.; Wei, Z. Large herbivore-induced changes in phytogenic hillocks: Links to soil and windblown sediment on the desert steppe in China. *Ecol. Res.* **2018**, *33*, 889–899. [\[CrossRef\]](#)
- Zhao, H.L.; Zhou, R.L.; Zhang, T.H.; Zhao, X.Y. Effects of desertification on soil and crop growth properties in Horqin sandy cropland of Inner Mongolia, north China. *Soil Tillage Res.* **2006**, *87*, 175–185. [\[CrossRef\]](#)
- Wan, D.; Mu, G.; Jin, Z.; Lei, J. The effects of oasis on aeolian deposition under different weather conditions: A case study at the southern margin of the Taklimakan desert. *Environ. Earth Sci.* **2013**, *68*, 103–114. [\[CrossRef\]](#)
- Fang, J. Variability in condensation water and its determinants in arid regions of north-western China. *Ecohydrology* **2020**, *13*, 1–12. [\[CrossRef\]](#)
- Zhang, Z.; Huisingh, D. Combating desertification in China: Monitoring, control, management and revegetation. *J. Clean. Prod.* **2018**, *182*, 765–775. [\[CrossRef\]](#)
- Zhou, C.H.; Zhao, L.Z.; Wang, A.Q.; Chen, T.H.; He, H.P. Current fundamental and applied research into clay minerals in China. *Appl. Clay Sci.* **2016**, *119*, 3–7.
- Yu, B.; Dong, H.; Jiang, H.; Lv, G.; Eberl, D.; Li, S.; Kim, J. The role of clay minerals in the preservation of organic matter in sediments of qinghai lake, NW China. *Clays Clay Miner.* **2009**. [\[CrossRef\]](#)
- Qi, Y.; Chen, T.; Shukla, M.K.; Chang, Q. Using soil minerals to investigate desert expansion in northern Shaanxi Province, China. *Aeolian Res.* **2020**, *43*, 100577. [\[CrossRef\]](#)
- Zhao, W.; Liu, L.; Chen, J.; Ji, J. Geochemical characterization of major elements in desert sediments and implications for the Chinese loess source. *Sci. China Earth Sci.* **2019**, *62*, 1428–1440. [\[CrossRef\]](#)
- Batista, A.H.; Melo, V.F.; Gilkes, R. Scanning and transmission analytical electron microscopy (STEM-EDX) identifies minor minerals and the location of minor elements in the clay fraction of soils. *Appl. Clay Sci.* **2017**, *135*, 447–456. [\[CrossRef\]](#)
- Chen, X.; Duan, Z.; Tan, M. Restoration Affect Soil Organic Carbon and Nutrients in Different Particle-size Fractions. *L. Degrad. Dev.* **2016**, *27*, 561–572. [\[CrossRef\]](#)
- Feng, X.; Qu, J.; Tan, L.; Fan, Q.; Niu, Q. Fractal features of sandy soil particle-size distributions during the rangeland desertification process on the eastern Qinghai-Tibet Plateau. *J. Soils Sediments* **2020**, *20*, 472–485. [\[CrossRef\]](#)
- Qi, Y.; Chen, T.; Pu, J.; Yang, F.; Shukla, M.K.; Chang, Q. Response of soil physical, chemical and microbial biomass properties to land use changes in fixed desertified land. *Catena* **2018**, *160*, 339–344. [\[CrossRef\]](#)

21. Li, D.; Wang, X.; Lou, J.; Liu, W.; Li, H.; Ma, W.; Jiao, L. Heterogeneity and loss of soil nutrient elements under aeolian processes in the Otindag Desert, China. *Aeolian Res.* **2018**, *30*, 48–53. [\[CrossRef\]](#)
22. Peng, F.; Xue, X.; You, Q.; Huang, C.; Dong, S.; Liao, J.; Duan, H.; Tsunekawa, A.; Wang, T. Changes of soil properties regulate the soil organic carbon loss with grassland degradation on the Qinghai-Tibet Plateau. *Ecol. Indic.* **2018**, *93*, 572–580. [\[CrossRef\]](#)
23. Zhang, Y.; Chun, X.; Zhou, H.; Zhang, Y.; Huang, S.; Wang, X. Particle size characteristics of surface sediments and their environmental significance: A comparative study of deserts in arid western Inner Mongolia, China. *Environ. Earth Sci.* **2020**, *79*. [\[CrossRef\]](#)
24. Liu, Q.; Zhao, Y.; Zhang, X.; Buyantuev, A.; Niu, J.; Wang, X. Spatiotemporal patterns of desertification dynamics and desertification effects on ecosystem services in the Mu Us Desert in China. *Sustainability* **2018**, *10*, 589. [\[CrossRef\]](#)
25. Li, J.; Tong, X.; Awasthi, M.K.; Wu, F.; Ha, S.; Ma, J.; Sun, X.; He, C. Dynamics of soil microbial biomass and enzyme activities along a chronosequence of desertified land revegetation. *Ecol. Eng.* **2018**. [\[CrossRef\]](#)
26. Zhang, J.; Wu, B.; Li, Y.; Yang, W.; Lei, Y.; Han, H.; He, J. Biological soil crust distribution in *Artemisia ordosica* communities along a grazing pressure gradient in Mu Us Sandy Land, Northern China. *J. Arid Land* **2013**. [\[CrossRef\]](#)
27. Wijewardane, N.K.; Ge, Y.; Wills, S.; Libohova, Z. Predicting Physical and Chemical Properties of US Soils with a Mid-Infrared Reflectance Spectral Library. *Soil Sci. Soc. Am. J.* **2018**. [\[CrossRef\]](#)
28. Meihuan, Y.; Mingming, C.; Zhu, Z. Soil Physical and Chemical Properties in the Process of Desertification on the Southeastern Edge of Mu Us Sandy Land. *Bull. Soil Water Conserv.* **2010**, *30*, 169–174.
29. Zhou, H.; Gao, Y.; Jia, X.; Wang, M.; Ding, J.; Cheng, L.; Bao, F.; Wu, B. Network analysis reveals the strengthening of microbial interaction in biological soil crust development in the Mu Us Sandy Land, northwestern China. *Soil Biol. Biochem.* **2020**. [\[CrossRef\]](#)
30. Xie, Y.; Qiu, K.; Xu, D.; Shi, X.; Qi, T.; Pott, R. Spatial heterogeneity of soil and vegetation characteristics and soil-vegetation relationships along an ecotone in Southern Mu Us Sandy Land, China. *J. Soils Sediments* **2015**. [\[CrossRef\]](#)
31. Zhang, C.; Shen, Y.; Li, Q.; Jia, W.; Li, J.; Wang, X. Sediment grain-size characteristics and relevant correlations to the aeolian environment in China's eastern desert region. *Sci. Total Environ.* **2018**, *627*, 586–599. [\[CrossRef\]](#)
32. Hu, F.; Yang, X.; Li, H. Origin and morphology of barchan and linear clay dunes in the Shuhongtu Basin, Alashan Plateau, China. *Geomorphology* **2019**, *339*, 114–126. [\[CrossRef\]](#)
33. Liu, Q.; Liu, G.; Huang, C.; Li, H. Remote Sensing Monitoring of Surface Characteristics in the Badain Jaran, Tengger, and Ulan Buh Deserts of China. *Chin. Geogr. Sci.* **2019**, *29*, 151–165. [\[CrossRef\]](#)
34. Lou, J.; Wang, X.; Zhu, B.; Li, D.; Jiao, L.; Ma, W.; Cai, D. The potential effects of aeolian processes on the vegetation in a semiarid area: Geochemical evidence from plants and soils. *Arab. J. Geosci.* **2018**, *11*. [\[CrossRef\]](#)
35. Shen, Z.; Caquineau, S.; Cao, J.; Zhang, X.; Han, Y.; Gaudichet, A.; Gomes, L. Mineralogical characteristics of soil dust from source regions in northern China. *Particuology* **2009**, *7*, 507–512. [\[CrossRef\]](#)
36. He, M.; Dijkstra, F.A.; Zhang, K.; Tan, H.; Zhao, Y.; Li, X. Influence of life form, taxonomy, climate, and soil properties on shoot and root concentrations of 11 elements in herbaceous plants in a temperate desert. *Plant Soil* **2016**, *398*, 339–350. [\[CrossRef\]](#)
37. Su, Y.Z.; Yang, R.; Liu, W.J.; Wang, X.F. Evolution of soil structure and fertility after conversion of native sandy desert soil to irrigated cropland in arid region, China. *Soil Sci.* **2010**, *175*, 246–254. [\[CrossRef\]](#)
38. Su, Y.Z.; Zhao, H.L.; Zhang, T.H.; Zhao, X.Y. Soil properties following cultivation and non-grazing of a semi-arid sandy grassland in northern China. *Soil Tillage Res.* **2004**, *75*, 27–36. [\[CrossRef\]](#)
39. Su, Y.Z.; Zhao, H.L.; Zhao, W.Z.; Zhang, T.H. Fractal features of soil particle size distribution and the implication for indicating desertification. *Geoderma* **2004**, *122*, 43–49. [\[CrossRef\]](#)
40. Li, Y.; Chen, Y.; Wang, S.; Huang, W.; Zhang, J. Effects of land-use changes on organic carbon in bulk soil and associated physical fractions in China's Horqin Sandy Grassland. *Sci. Cold Arid Reg.* **2015**, *7*, 50–58. [\[CrossRef\]](#)
41. Li, H.; Zeng, F.; Gui, D.; Lei, J. Characteristics of soil environment variation in oasis-desert ecotone in the process of oasis growth. In Proceedings of the International Conference on Computer and Computing Technologies in Agriculture, Beijing, China, 29–31 October 2011; Volume 344, pp. 321–334. [\[CrossRef\]](#)
42. Yu, X.; Grace, M.; Zou, Y.; Yu, X.; Lu, X.; Wang, G. Surface sediments in the marsh-sandy land transitional area: Sandification in the western Songnen Plain, China. *PLoS ONE* **2014**, *9*, e99715. [\[CrossRef\]](#)
43. Taghizadeh-Mehrjardi, R.; Akbarzadeh, A. Soil physico-chemical, mineralogical, and micromorphological changes due to desertification processes in Yazd region, Iran. *Arch. Agron. Soil Sci.* **2014**, *60*, 487–506. [\[CrossRef\]](#)
44. Hameed, A.; Raja, P.; Ali, M.; Upreti, N.; Kumar, N.; Tripathi, J.K.; Srivastava, P. Micromorphology, clay mineralogy, and geochemistry of calcic-soils from western Thar Desert: Implications for origin of palygorskite and southwestern monsoonal fluctuations over the last 30 ka. *Catena* **2018**, *163*, 378–398. [\[CrossRef\]](#)
45. Zhang, J.Y.; Gu, P.F.; Li, L.Y.; Zong, L.Y.; Zhao, W.J. Changes of soil particle size fraction along a chronosequence in sandy desertified land: A fundamental process for ecosystem succession and ecological restoration. *J. Soils Sediments* **2016**, *16*, 2651–2656. [\[CrossRef\]](#)
46. Zhang, J.; Zuo, X.; Zhou, X.; Lv, P.; Lian, J.; Yue, X. Long-term grazing effects on vegetation characteristics and soil properties in a semiarid grassland, northern China. *Environ. Monit. Assess.* **2017**, *189*. [\[CrossRef\]](#)
47. Deng, J.; Li, J.; Deng, G.; Zhu, H.; Zhang, R. Fractal scaling of particle-size distribution and associations with soil properties of Mongolian pine plantations in the Mu Us Desert, China. *Sci. Rep.* **2017**, *7*, 6742. [\[CrossRef\]](#)

48. Chen, X.; Duan, Z.; Luo, T. Changes in soil quality in the critical area of desertification surrounding the Ejina Oasis, Northern China. *Environ. Earth Sci.* **2014**, *72*, 2643–2654. [\[CrossRef\]](#)
49. Tang, Z.; An, H.; Deng, L.; Wang, Y.; Zhu, G.; Shangguan, Z. Effect of desertification on productivity in a desert steppe. *Sci. Rep.* **2016**, *6*, 27839. [\[CrossRef\]](#)
50. Zhang, J.; Hou, P. Soil quality change during reversal of desertification in agro-pastoral transition zone of northern China. *Adv. Mat. Res.* **2012**, *599*, 859–864. [\[CrossRef\]](#)
51. Cao, C.; Jiang, D.; Teng, X.; Jiang, Y.; Liang, W.; Cui, Z. Soil chemical and microbiological properties along a chronosequence of Caragana microphylla Lam. plantations in the Horqin sandy land of Northeast China. *Appl. Soil Ecol.* **2008**, *40*, 78–85. [\[CrossRef\]](#)
52. Zou, X.; Li, J.; Cheng, H.; Wang, J.; Zhang, C.; Kang, L.; Liu, W.; Zhang, F. Spatial variation of topsoil features in soil wind erosion areas of northern China. *Catena* **2018**, *167*, 429–439. [\[CrossRef\]](#)
53. Yang, Y.Y.; Liu, L.Y.; Shi, P.J.; Zhang, G.M.; Qu, Z.Q.; Tang, Y.; Lei, J.; Wen, H.M.; Xiong, Y.Y.; Wang, J.P.; et al. Morphology, spatial pattern and sediment of Nitraria tangutorum nebkhas in barchans interdune areas at the southeast margin of the Badain Jaran Desert, China. *Geomorphology* **2015**, *232*, 182–192. [\[CrossRef\]](#)
54. Shuai, Z.; Ding, G.; Yu, M.; Gao, G.; Zhao, Y. Effect of Straw Checkerboards on Wind Proofing, Sand Fixation, and Ecological Restoration in Shifting Sandy Land. *Int. J. Environ. Res. Public Health* **2018**, *123*, 184. [\[CrossRef\]](#)
55. Dai, Y.; Dong, Z.; Li, H.; He, Y.; Li, J.; Guo, J. Geomorphology Effects of checkerboard barriers on the distribution of aeolian sandy soil particles and soil organic carbon. *Geomorphology* **2019**, *338*, 79–87. [\[CrossRef\]](#)
56. Wang, J.; Wang, R. The physical and chemical properties of soil crust in straw checkerboards with different ages in the Mu Us Sandland, Northern China. *Sustainability* **2019**, *11*, 4755. [\[CrossRef\]](#)
57. Xu, T.T.; Dong, Z.; Li, H.L.; Shao, S.X.; Wang, L.Q. Distribution of soil particle size and soil organic carbon in dunes of checkerboard barriers with different setting years. *Res. Environ. Sci.* **2014**, *27*, 628–634. [\[CrossRef\]](#)
58. Li, D.; Xu, D. Sand fixation function response to climate change and land use in northern China from 1981 to 2015. *Aeolian Res.* **2019**, *40*, 23–33. [\[CrossRef\]](#)
59. Ning, H.; Xia, X.; Ding, T. Numerical simulation of wind sand movement in straw checkerboard barriers. *Eur. Phys. J. E* **2013**, *36*. [\[CrossRef\]](#)
60. Wang, Y.; Yuan, W.; Ding, G. Concave surface features and grain-size characteristics in polylactic acid sand barrier. *Arid Land Geogr.* **2020**, *43*, 671–678. [\[CrossRef\]](#)
61. Ding, Y.; Gao, Y.; Wang, J. Effects of Biodegradable Poly Lactic Acid Sand Barriers on Surface Sediment Grain-size Characteristics at Sand Dunes. *J. Desert Res.* **2018**, *38*. [\[CrossRef\]](#)
62. Zhongju, M.; Ren, X.; Yong, G. Effects of PLA Sand Barriers on Soil Fractal Dimension. *Chin. J. Soil Sci.* **2014**, *45*, 10–12. [\[CrossRef\]](#)
63. Liu, X.; Xie, Y.; Zhou, D.; Li, X.; Ding, J.; Wu, X.; Wang, J.; Hai, C. Soil grain-size characteristics of nitraria tangutorum nebkhas with different degrees of vegetation coverage in a desert-oasis ecotone. *Polish J. Environ. Stud.* **2020**, *29*, 3703–3714. [\[CrossRef\]](#)
64. Zhang, J.; Chang, Q.R.; Qi, Y.B. Fractal characteristics of soil under ecological restoration in the agro-pastoral transition zone of northern China. *N. Z. J. Agric. Res.* **2009**, *52*, 471–476. [\[CrossRef\]](#)
65. Gao, G.L.; Ding, G.D.; Wu, B.; Zhang, Y.Q.; Qin, S.G.; Zhao, Y.Y.; Bao, Y.F.; Liu, Y.D.; Wan, L.; Deng, J.F. Fractal scaling of particle size distribution and relationships with topsoil properties affected by biological soil crusts. *PLoS ONE* **2014**, *9*, e88559. [\[CrossRef\]](#) [\[PubMed\]](#)
66. Gao, G.L.; Ding, G.D.; Zhao, Y.Y.; Wu, B.; Zhang, Y.Q.; Qin, S.G.; Bao, Y.F.; Yu, M.H.; Liu, Y.D. Fractal approach to estimating changes in soil properties following the establishment of Caragana korshinskii shelterbelts in Ningxia, NW China. *Ecol. Indic.* **2014**, *43*, 236–243. [\[CrossRef\]](#)
67. Deng, J.; Ma, C.; Yu, H. Different soil particle-size classification systems for calculating volume fractal dimension—a case study of Pinus sylvestris var. Mongolica in Mu Us Sandy Land, China. *Appl. Sci.* **2018**, *8*, 1872. [\[CrossRef\]](#)
68. Zhang, J.; Jia, G.; Liu, Z.; Wang, D.; Yu, X. Populus simonii Carr. Reduces wind erosion and improves soil properties in Northern China. *Forests* **2019**, *10*, 315. [\[CrossRef\]](#)
69. Zhang, Y.G.; Xu, Z.W.; Jiang, D.M.; Jiang, Y. Soil exchangeable base cations along a chronosequence of Caragana microphylla plantation in a semi-arid sandy land, China. *J. Arid Land* **2013**, *5*, 42–50. [\[CrossRef\]](#)
70. Fan, B.; Zhang, A.; Yang, Y.; Ma, Q.; Li, X.; Zhao, C. Long-Term effects of xerophytic shrub haloxylon ammodendron plantations on soil properties and vegetation dynamics in northwest China. *PLoS ONE* **2016**, *11*, e0168000. [\[CrossRef\]](#) [\[PubMed\]](#)
71. Wang, Y.; Zhao, Y.; Li, S.; Shen, F.; Jia, M.; Zhang, J.; Xu, X.; Lei, J. Soil aggregation formation in relation to planting time, water salinity, and species in the Taklimakan Desert Highway shelterbelt. *J. Soils Sediments* **2018**, *18*, 1466–1477. [\[CrossRef\]](#)
72. Li, Y.; Li, Z.; Wang, Z.; Wang, W.; Jia, Y.; Tian, S. *Impacts of Artificially Planted Vegetation on the Ecological Restoration of Movable Sand Dunes in the Mugetan Desert, Northeastern Qinghai-Tibet Plateau*; Elsevier: Amsterdam, The Netherlands, 2017; Volume 32, ISBN 1827487658.
73. Wang, X.P.; Li, X.R.; Xiao, H.L.; Pan, Y.X. Evolutionary characteristics of the artificially revegetated shrub ecosystem in the Tengger Desert, northern China. *Ecol. Res.* **2006**, *21*, 415–424. [\[CrossRef\]](#)
74. Wang, M.; Dong, Z.; Luo, W.; Lu, J.; Li, J. Spatial variability of vegetation characteristics, soil properties and their relationships in and around China's Badain Jaran Desert. *Environ. Earth Sci.* **2015**, *74*, 6847–6858. [\[CrossRef\]](#)
75. Zhenghu, D.; Honglang, X.; Zhibao, D.; Gang, W.; Drake, S. Morphological, physical and chemical properties of aeolian sandy soils in northern China. *J. Arid Environ.* **2007**, *68*, 66–76. [\[CrossRef\]](#)

76. Yimin, W.; Liu, K.; Qu, J. Effects of Sand Barriers on Vegetation and Soil Nutrient in Sand Dunes. *J. Desert Res.* **2019**, *39*, 56–65. [\[CrossRef\]](#)
77. Baoying, N.; Jianxia, M.; Zhide, J.; Chun, C.; Xinli, Z.; Jingliang, L. Evolution Characteristics and Development Trends of Sand Barriers. *J. Resour. Ecol.* **2017**, *8*, 398–404. [\[CrossRef\]](#)
78. Yuan, J.; Ye, C.; Luo, L.; Pei, X.; Yang, Q.; Chen, J.; Liao, B. Sand fixation property and erosion control through new cellulose-based curing agent on sandy slopes under rainfall. *Bull. Eng. Geol. Environ.* **2020**, *79*, 4051–4061. [\[CrossRef\]](#)
79. Zhao, L.; Li, X.; Wang, Z.; Qi, J.; Zhang, W.; Wang, Y.; Liu, Y. A new strain of *Bacillus tequilensis* CGMCC 17603 isolated from biological soil crusts: A promising sand-fixation agent for desertification control. *Sustainability* **2019**, *11*, 6501. [\[CrossRef\]](#)
80. Peng, C.; Zheng, J.; Huang, S.; Li, S.; Li, D.; Cheng, M.; Liu, Y. Application of sodium alginate in induced biological soil crusts: Enhancing the sand stabilization in the early stage. *J. Appl. Phycol.* **2017**, *29*, 1421–1428. [\[CrossRef\]](#)
81. Zhou, C.; Zhao, S.; Huang, W.; Li, D.; Liu, Z. Study on the stabilization mechanisms of clayey slope surfaces treated by spraying with a new soil additive. *Appl. Sci.* **2019**, 1245. [\[CrossRef\]](#)
82. Zhou, C.; Ge, X.; Huang, W.; Li, D.; Liu, Z. Effects of aqua-dispersing nano-binder on clay conductivity at different temperatures. *Sustainability* **2019**, *11*, 4859. [\[CrossRef\]](#)
83. Zang, Y.; Gong, W.; Xie, H.; Du, Z.; Liu, B.; Chen, H. Evaluation and mechanism of anionic waterborne polyurethane dispersion for chemical sand stabilisation. *Plast. Rubber Compos.* **2016**, *45*, 270–276. [\[CrossRef\]](#)
84. Liu, J.; Shi, B.; Lu, Y.; Jiang, H.; Huang, H.; Wang, G.; Kamai, T. Effectiveness of a new organic polymer sand-fixing agent on sand fixation. *Environ. Earth Sci.* **2012**, *65*, 589–595. [\[CrossRef\]](#)
85. Onyejekwe, S.; Ghataora, G.S. Soil stabilization using proprietary liquid chemical stabilizers: Sulphonated oil and a polymer. *Bull. Eng. Geol. Environ.* **2015**, *74*, 651–665. [\[CrossRef\]](#)
86. Ma, G.; Feng, E.; Ran, F.; Dong, Z.; Lei, Z. Preparation and Sand-Fixing Property of a Novel and Eco-friendly Organic-Inorganic Composite. *Polym. Plast. Technol. Eng.* **2015**, *54*, 703–710. [\[CrossRef\]](#)
87. Liu, J.; Shi, B.; Jiang, H.; Bae, S.; Huang, H. Improvement of water-stability of clay aggregates admixed with aqueous polymer soil stabilizers. *Catena* **2009**, *77*, 175–179. [\[CrossRef\]](#)
88. Ajalloeian, R.; Matinmanesh, H.; Abtahi, S.M.; Rowshanzamir, M. Effect of polyvinyl acetate grout injection on geotechnical properties of fine sand. *Geomech. Geoengin.* **2013**, *8*, 86–96. [\[CrossRef\]](#)
89. Wang, N.; Xie, J.; Han, J. A sand control and development model in sandy land based on mixed experiments of arsenic sandstone and sand: A case study in mu us sandy land in China. *Chin. Geogr. Sci.* **2013**, *23*, 700–707. [\[CrossRef\]](#)
90. Sun, Y.; Zhang, N.; Yan, J.; Zhang, S. Effects of soft rock and biochar applications on millet (*Setaria italica* L.) crop performance in sandy soil. *Agronomy* **2020**, *10*, 669. [\[CrossRef\]](#)
91. Saiedi, N.; Besalatpour, A.A.; Shirani, H.; Abbaszadeh Dehaji, P.; Esfandiarpour, I.; Faramarzi, M. Aggregation and fractal dimension of aggregates formed in sand dunes stabilized by PistachioPAM and PistachioPVAc mulches. *Eur. J. Soil Sci.* **2017**, *68*, 783–791. [\[CrossRef\]](#)
92. Liu, J.; Shi, B.; Jiang, H.; Huang, H.; Wang, G.; Kamai, T. Research on the stabilization treatment of clay slope topsoil by organic polymer soil stabilizer. *Eng. Geol.* **2011**, *117*, 114–120. [\[CrossRef\]](#)
93. Zezin, A.B.; Mikheikin, S.V.; Rogacheva, V.B.; Zansokhova, M.F.; Sybachin, A.V.; Yaroslavov, A.A. Polymeric stabilizers for protection of soil and ground against wind and water erosion. *Adv. Colloid Interface Sci.* **2015**, *226*, 17–23. [\[CrossRef\]](#)
94. Zhang, L.; Jing, Y.; Chen, G.; Wang, X.; Zhang, R. Improvement of physical and hydraulic properties of desert soil with amendment of different biochars. *J. Soils Sediments* **2019**. [\[CrossRef\]](#)
95. Park, C.H.; Li, X.R.; Zhao, Y.; Jia, R.L.; Hur, J.S. Rapid development of cyanobacterial crust in the field for combating desertification. *PLoS ONE* **2017**, *12*, 1–20. [\[CrossRef\]](#) [\[PubMed\]](#)
96. Liao, C.; Li, H.; Lv, G.; Tian, J.; Xu, Y. Effects of ecological restoration on soil properties of the aeolian sandy land around Lhasa, southern Tibetan Plateau. *Ecosphere* **2020**, *11*. [\[CrossRef\]](#)
97. Zhang, T.H.; Su, Y.Z.; Cui, J.Y.; Zhang, Z.H.; Chang, X.X. A leguminous shrub (*Caragana microphylla*) in semiarid sandy soils of north China. *Pedosphere* **2006**, *16*, 319–325. [\[CrossRef\]](#)
98. Li, Q.; Jia, Z.; Liu, T.; Feng, L.; He, L. Effects of different plantation types on soil properties after vegetation restoration in an alpine sandy land on the Tibetan Plateau, China. *J. Arid Land* **2017**, *9*, 200–209. [\[CrossRef\]](#)
99. Zhao, H.L.; Guo, Y.R.; Zhou, R.L.; Drake, S. Biological soil crust and surface soil properties in different vegetation types of Horqin Sand Land, China. *Catena* **2010**, *82*, 70–76. [\[CrossRef\]](#)
100. Xue mei, W.; Lijun, C. Analysis of Soil Particle Size of Typical Plant Communities in Desert Ecotone on Northern Margin of Tarim Basin. *Southwest China J. Agric. Sci.* **2019**, *32*, 2848–2855.
101. Qu, Y.; Zhang, Z. The design and application of non-pressure infiltrating irrigation in desertification control. *Sustainability* **2020**, *12*, 1547. [\[CrossRef\]](#)
102. Chepil, W.S. Factors that influence clod structure and erodibility of soil by wind: IV. Sand, silt, and clay. *Soil Sci.* **1955**, *80*, 155–162. [\[CrossRef\]](#)
103. Liu, L.Y.; Li, X.Y.; Shi, P.J.; Gao, S.Y.; Wang, J.H.; Ta, W.Q.; Song, Y.; Liu, M.X.; Wang, Z.; Xiao, B.L. Wind erodibility of major soils in the farming-pastoral ecotone of China. *J. Arid Environ.* **2007**, *68*, 611–623. [\[CrossRef\]](#)
104. López, M.V. Wind erosion in agricultural soils: An example of limited supply of particles available for erosion. *Catena* **1998**, *33*, 17–28. [\[CrossRef\]](#)

105. Yang, L.R.; Yue, L.P.; Li, Z.P. The influence of dry lakebeds, degraded sandy grasslands and abandoned farmland in the arid inland of northern China on the grain size distribution of East Asian aeolian dust. *Environ. Geol.* **2008**, *53*, 1767–1775. [\[CrossRef\]](#)
106. Bei, S.; Zining, Z. Research Progress on Soil Erodibility. *Chin. J. Soil Sci.* **2016**, *47*. [\[CrossRef\]](#)
107. Wang, H.; Jia, X.; Li, K.; Li, Y. Horizontal wind erosion flux and potential dust emission in arid and semiarid regions of China: A major source area for East Asia dust storms. *Catena* **2015**, *133*, 373–384. [\[CrossRef\]](#)
108. Krishnappan, B.G.; Burrell, B.C. Using mosand to mitigate the desertification of minqin oasis, Gansu province, China. *Can. J. Civ. Eng.* **2012**. [\[CrossRef\]](#)
109. Nan, L.; Du, L.; Zhan, X. Advances in Study on Soil Erodibility for Wind Erosion. *Soils* **2014**, *46*, 204–211. [\[CrossRef\]](#)
110. Karlen, D.L.; Mausbach, M.J.; Doran, J.W.; Cline, R.G.; Harris, R.F.; Schuman, G.E. Soil Quality: A Concept, Definition, and Framework for Evaluation (A Guest Editorial). *Soil Sci. Soc. Am. J.* **1997**. [\[CrossRef\]](#)
111. Laishram, J.; Saxena, K.G.; Maikhuri, R.K.; Rao, K.S. Soil Quality and Soil Health: A Review. *Int. J. Ecol. Environ. Sci.* **2012**, *38*, 19–37.
112. Yang, Q.; Li, Z.; Lu, X.; Duan, Q.; Huang, L.; Bi, J. A review of soil heavy metal pollution from industrial and agricultural regions in China: Pollution and risk assessment. *Sci. Total Environ.* **2018**, *642*, 690–700. [\[CrossRef\]](#)
113. Bai, Z.; Caspari, T.; Gonzalez, M.R.; Batjes, N.H.; Mäder, P.; Bünemann, E.K.; de Goede, R.; Brussaard, L.; Xu, M.; Ferreira, C.S.S.; et al. Effects of agricultural management practices on soil quality: A review of long-term experiments for Europe and China. *Agric. Ecosyst. Environ.* **2018**. [\[CrossRef\]](#)
114. Wang, B.; Xue, S.; Liu, G.B.; Zhang, G.H.; Li, G.; Ren, Z.P. Changes in soil nutrient and enzyme activities under different vegetations in the Loess Plateau area, Northwest China. *Catena* **2012**. [\[CrossRef\]](#)
115. Gao, L.; Bowker, M.A.; Xu, M.; Sun, H.; Tuo, D.; Zhao, Y. Biological soil crusts decrease erodibility by modifying inherent soil properties on the Loess Plateau, China. *Soil Biol. Biochem.* **2017**, *105*, 49–58. [\[CrossRef\]](#)
116. Shuai, Z.; Ding, G.; Gao, G. Effects of straw checkerboard barrier in different setting years on ecological restoration. *Sci. Soil Water Conserv.* **2018**, *16*, 10–15.
117. Xu, B.; Zhang, J.; Huang, N.; Gong, K.; Liu, Y. Characteristics of Turbulent Aeolian Sand Movement Over Straw Checkerboard Barriers and Formation Mechanisms of Their Internal Erosion Form. *J. Geophys. Res. Atmos.* **2018**, *123*, 6907–6919. [\[CrossRef\]](#)
118. Turgeon, K.; Robillard, A.; Grégoire, J.; Duclos, V.; Kramer, D.L. Functional connectivity from a reef fish perspective: Behavioral tactics for moving in a fragmented landscape. *Ecology* **2010**. [\[CrossRef\]](#)
119. Wang, R.D.; Dang, X.H.; Gao, Y.; Yang, X.; Liang, Y.M.; Qi, S.; Zhao, C. Alternated desorption-absorption accelerated aging of *Salix psammophila* sand barrier. *BioResources* **2020**, *15*, 6696–6713. [\[CrossRef\]](#)
120. Tang, F.K.; Cui, M.; Lu, Q.; Liu, Y.G.; Guo, H.Y.; Zhou, J.X. Effects of vegetation restoration on the aggregate stability and distribution of aggregate-associated organic carbon in a typical karst gorge region. *Solid Earth* **2016**, *7*, 141–151. [\[CrossRef\]](#)
121. Huang, W.; Liu, Z.; Zhou, C.; Yang, X. Enhancement of soil ecological self-repair using a polymer composite material. *Catena* **2020**. [\[CrossRef\]](#)
122. Park, C.H.; Li, X.; Jia, R.L.; Hur, J.S. Effects of Superabsorbent Polymer on Cyanobacterial Biological Soil Crust Formation in Laboratory. *Arid Land Res. Manag.* **2015**, *29*, 55–71. [\[CrossRef\]](#)
123. Li, J.; Gilhooly, W.P.; Okin, G.S.; Blackwell, J. Abiotic processes are insufficient for fertile island development: A 10-year artificial shrub experiment in a desert grassland. *Geophys. Res. Lett.* **2017**, *44*, 2245–2253. [\[CrossRef\]](#)
124. An, H.; Li, Q.L.; Yan, X.; Wu, X.Z.; Liu, R.T.; Fang, Y. Desertification control on soil inorganic and organic carbon accumulation in the topsoil of desert grassland in Ningxia, northwest China. *Ecol. Eng.* **2019**, *127*, 348–355. [\[CrossRef\]](#)
125. Wang, X.; Wang, T.; Dong, Z.; Liu, X.; Qian, G. Nebkha development and its significance to wind erosion and land degradation in semi-arid northern China. *J. Arid Environ.* **2006**, *65*, 129–141. [\[CrossRef\]](#)
126. Li, X.; Vogeler, I.; Schwendenmann, L. Soil aggregation and soil fraction associated carbon under different vegetation types in a complex landscape. *Soil Res.* **2019**, *57*, 215–227. [\[CrossRef\]](#)
127. Li, B.; Gao, J.; Wang, X.; Ma, L.; Cui, Q.; Vest, M. Effects of biological soil crusts on water infiltration and evaporation Yanchi Ningxia, Maowusu Desert, China. *Int. J. Sediment Res.* **2016**, *31*, 311–323. [\[CrossRef\]](#)
128. Huo, A.; Wang, X.; Guan, W.; Zhong, J.; Yi, X.; Wen, Y. Soil physico-chemical properties and their effects on populus euphratica growth in desertification areas. *Acta Scientific Agric.* **2018**, *2*, 2–9.
129. Wang, Y.; Zhou, L. Assessment of the coordination ability of sustainable social-ecological systems development based on a set pair analysis: A case study in Yanchi County, China. *Sustainability* **2016**, *8*, 733. [\[CrossRef\]](#)
130. Li, H.; Zhan, H.X.; Xu, H. Fractal features of soil particles under different plant communities in the yimeng mountain of China. *Appl. Ecol. Environ. Res.* **2019**, *17*, 15731–15743. [\[CrossRef\]](#)
131. Wei, X.; Li, X.; Wei, N. Fractal features of soil particle size distribution in layered sediments behind two check dams: Implications for the Loess Plateau, China. *Geomorphology* **2016**, *266*, 133–145. [\[CrossRef\]](#)
132. Xiao, L.; Xue, S.; Liu, G.B.; Zhang, C. Fractal features of soil profiles under different land use patterns on the Loess Plateau, China. *J. Arid Land* **2014**, *6*, 550–560. [\[CrossRef\]](#)